Journal of Physics: Conference Series **500** (2014) 192016 doi:10.1088/1742-6596/500/19/192016

Strength and sintering effects at ejection of explosively driven sand

A D Resnyansky and S A Weckert

Weapons and Countermeasures Division, DSTO, PO Box 1500, Edinburgh SA 5111, Australia

E-mail: anatoly.resnyansky@dsto.defence.gov.au

Abstract. A description of the response of sand to extreme loads is very important for the evaluation of the sand ejecta impact effects on various targets. Sand is a complex material to simulate because of its porosity where the inter-phase equilibrium is hard to achieve under transient shock wave loading. A previously developed two-phase model with strength has been implemented in CTH and applied to sand. The shock response of the sand, including the Hugoniot abnormality known from the literature for highly porous silica, is adequately described with the material model. The sand unloading effects appearing as the ejecta are observed in the present work using dynamic flash X-ray of an aluminium target plate loaded by limestone sand ejecta from the detonation of a buried high explosive charge. The CTH modelling results compared with the flash X-ray images have demonstrated good agreement, particularly, in the description of momentum transfer to the target.

1. Introduction

Sand and soil ejection effects due to detonation of a buried high explosive (HE) charge are associated with the behavior of porous materials subject to the loading by shock and release waves. Previous studies have mainly observed after-test effects to a target [1,2]. A further advancement in the sand ejection observations was measurements of the momentum deposited onto a target including time-resolved observations [3,4]. These measurements, however, involved a significant inertial contribution from the momentum measurement device (e.g., pendulum). Dynamic observation of sand ejecta has been conducted in tests [5] using a flash X-ray technique. However, snapshots of the soil ejecta do not provide the inside-ejecta distribution of mass and velocity, enabling one to trace only the ejecta shape. Therefore, the time resolved deposition of momentum to a potential target is difficult to evaluate, whereas this is particularly important for the assessment of the shock wave effects in the target.

The present work involves the experimental and numerical analysis of the dynamic response of a target subject to loading from the sand ejecta. The experiments have recorded the flash X-ray images of a deforming plate, loaded by the sand ejecta from a buried HE charge, in a quasi two-dimensional (2D) set-up. For moderate stand-off distances between the soil and target, where the gaseous products and the air within a porous material are in velocity equilibrium with the soil/sand particles, the two-phase model [6] can be employed for description of the shock response of the porous material. An effect of possible strength change of the condensed constituent of the material due to high-temperature effects during the loading by the detonation products is considered and is taken into account by the

introduction of a suitable constitutive equation. The model has been implemented in the CTH hydrocode and validated against the observed dynamic target deformation.

2. Experimental

The experimental assembly approximates a two-dimensional set-up in (x,y)-space. The loading is achieved by a 4x2 cm HE main charge with a 24 cm-extension of the charge in the z-direction. The main charge, sitting on a thick steel base, is initiated by a linear 3 mm thick charge initiated by an explosively lensed line wave generator (figure 1(a)). The explosive used for both the main charge and the linear charge is Primasheet 2000, an RDX based explosive. The charge is buried under a layer of sand with 4 cm overburden for the main charge. The average density of sand is 1.35 g/cm^3, and the sand is contained within a 10 mm-thick box forming the assembly shown in figure 1(b). After initiation, the detonation products and sand ejecta load the 4 mm thick target plate made from 6061-T6 aluminium, and the side view of the deforming target is projected onto a digital X-ray cassette. The two-dimensional schematic of the set-up representing the side view projected onto the X-ray cassette is shown in figure 1(c). The result is two flash X-ray images, separated in time, superimposed for each shot. The test series included four tests with a typical result for one of the tests shown in figure 1(d).

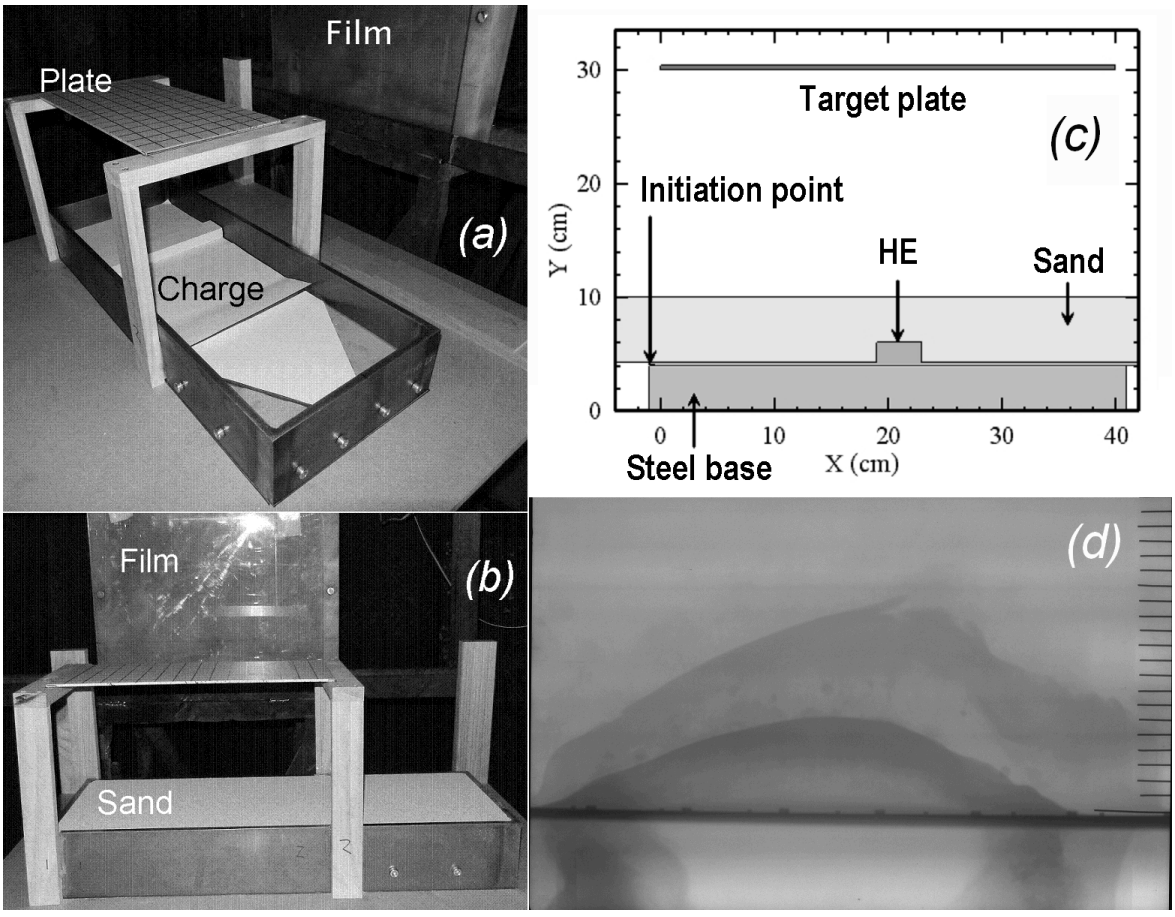

Figure 1. Experimental set-up involving a target plate subject to loading by sand ejecta from a buried high explosive charge (*a*-*b*). Two-dimensional schematic of the set-up (*c*) and the flash X-ray image (*d*) of the target plate (two exposures on the same film) for Test 2.

The time marks of the X-ray images relative to the detonation wave initiating the linear charge (shown as the initiation point in the schematic of figure 1(c)) are summarized in table 1. Specifically, Test 1 recorded the target images #4 and #8, Test 2 – #3 and #7, Test 3 – #1 and #5, and Test 4 – #2

and #6. For example, the image in figure 1(d) visualizing the target images #3 and #7 is taken from Test 2. When analyzing, the X-ray images have been flipped about the vertical axis in order to agree with the numerical set-up.

Table 1. Time marks of the flash X-ray images for the 4 tests.

#	1	2	3	4	5	6	7	8
Time, μs	340	380	380	412	440	440	480	540

The observation angle from the X-ray pulser head gives a horizontal divergence of approximately 10%. Markers, consisting of steel inserts along the plate edge at the front and rear, spaced at 50 mm, have been positioned on the target plate. These can be seen in the static image of the undeformed plate in figure 1(d). The markers have been used for the evaluation of the plate deformation and accuracy with the maximal error of the determined plate position being less than 9%.

3. Model

The two-phase porous material model with strength considers a porous material as a mixture of gaseous (first phase) and condensed (second phase) components. Strength for the first phase is ignored. The model [6] incorporates the conservation laws, the shear deformation rheological law, and the constitutive equations of the inter-phase exchange for mass, dilatation, heat, and shear strain work. The mass exchange between phases is neglected in the present case. The compaction kinetic is taken from [7] and the heat exchange kinetic from [6,8]. The shear strain rheology and strain work are only considered for the condensed phase (granular or consolidated compact) and the kinetic is determined from two yield limit points (for example, static, Y_s, and dynamic, Y_d) at two strain rates [6,8].

The model equations are closed with an equation of state (EOS) for each of the constituents in the form of internal energy against density, strain and entropy. Using the mixture additive rule for the internal energy, e, provides an EOS for the porous material. The thermodynamics rules allow us to calculate all dependent thermodynamic parameters by differentiation of e, including pressure, affinity of the Gibbs energies (the chemical potential), the compaction rate, shear stress, strain work exchange rate, temperature, and temperature imbalance.

The model has been complemented with a 'sintering' kinetic $d\xi/dt = f(\xi,T)$. The function f contains an energy activation term that initiates treatment of the sintering process and adapts the skin model formulated as the powder consolidation theory in [11]. As a result, the auxiliary parameter ξ manages consolidation, the transition from a low strength regime at room temperature to a high strength regime at a temperature where sintering of the condensed phase occurs.

The above stated version of the model has been implemented in the CTH hydrocode [9]. CTH is a multi-material, large deformation, strong shock wave, solid mechanics code developed at Sandia National Laboratories [10]. The present implementation involves modification of subroutines in Lagrangian and Eulerian parts of the CTH code [9] in the entries related to the cell thermodynamics at the Eulerian step (EOS implementation), the deviatoric stress calculations (the strength related constitutive equations implementation), and the extra variables update (the inter-phase exchange related constitutive equations implementation).

4. Modelling and comparison with experiments

The two-phase porous material model implemented in CTH was first tested using the plane impact set-up. The plane impact tests and corresponding Hugoniots are well known and the anomalous response of a highly porous material is one of the basic tests for a model. The available Hugoniot data for highly porous silica (ρ_0 = 0.4 g/cm^3) [12] demonstrate the clear abnormal response, which is summarized in figure 2. Results of the CTH calculations for the shock propagation using the present model are presented as a set of density profiles inside the sand sample impacted by a copper flyer plate

at velocity U_0 (6 set-ups with different U_0, the dashed line is the contact interface between the flyer plate and the target silica sample). The developed, nearly-stationary, calculated profiles are shown in figure 3. These were: 1 – U_0 = 0.5 km/s (0.15); 2 – U_0 = 1 km/s (0.4); 3 – U_0 = 3 km/s (4); 4 – U_0 = 5 km/s (10); 5 – U_0 = 7 km/s (20); and 6 – U_0 = 9 km/s (35). The corresponding pressure in GPa calculated behind the shock front is noted in parenthesis after the velocity value.

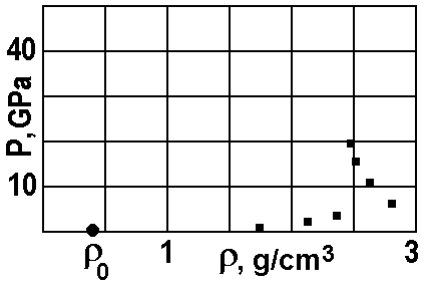

Figure 2. Experimental Hugoniot data points for a highly porous silica [12], ρ_0 = 0.4 g/cm^3.

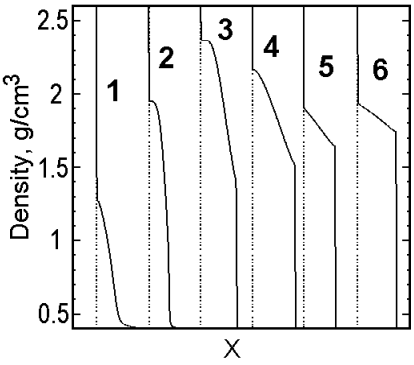

Figure 3. Density profiles in highly porous silica loaded by the shock waves with increasing pressure.

It is seen that the abnormal behaviour is well described by the model. The compaction and heat transfer kinetics have been taken from [7,8] with the normal thermo-mechanical characteristics for the polycrystalline quartz representing a condensed phase of the two-phase mixture.

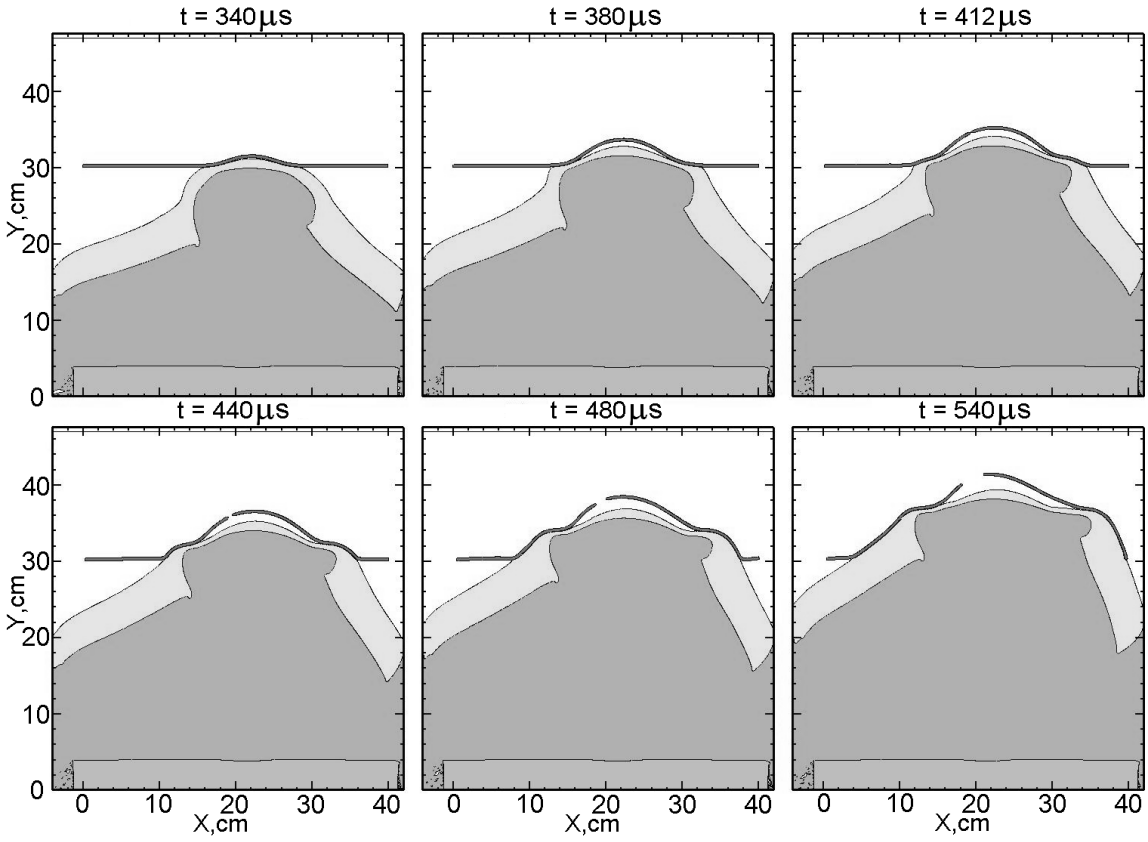

Figure 4. CTH calculation of the sand ejecta, loading an aluminium target plate.

Dry limestone sand (200 μm average particle size) was used in the present experiments with at least 96% purity calcium carbonate material and less than 0.3% moisture content. The model [6] applied to this material enabled us to conduct CTH calculations of the 2D-set-up in figure 1(c). Several options to characterise the strength of the condensed phase are considered. One calculation, using the sintering kinetic for the development of strength, plotted at the time marks of table 1 is shown in figure 4 with the dark grey region corresponding to detonation products and the light grey area for sand.

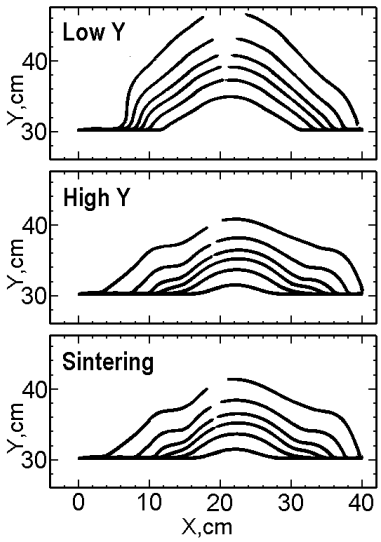

Figure 5. CTH calculations with the present model with three options for the yield limit of the condensed phase.

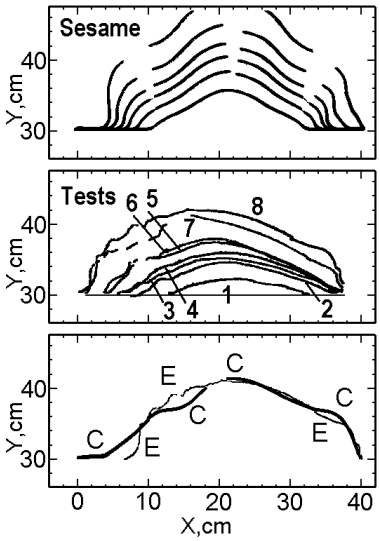

Figure 6. The Sesame model calculation, experimental plate contours, and comparison of the sintering calculation (C) with the experiment (E) at t = 540 μs.

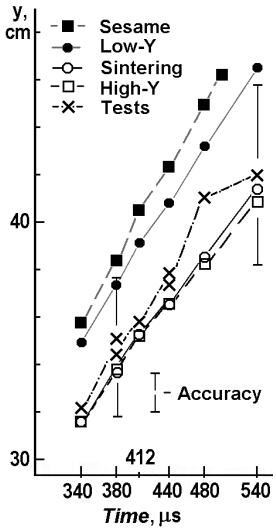

Figure 7. Vertical momentum transfer for the present CTH calculations and the experiment.

The concept of strength is somewhat speculative in porous materials because this property is mainly related to the granular material or consolidated compact. The use of the sintering kinetic derived from the theory [11] and to be detailed in a further publication is substantiated by comparison of the calculated sand ejecta [8] with experiment [5]. It was observed that the calculations [8] with the low yield limit (Y) condensed phase of sand describe large depth of burial (DOB) charge tests well along with the high-Y calculations for shallow DOB tests. From the analysis of the temperature fields inside the ejecta a longer high-temperature effect observed for the shallow DOB case suggests possible consolidation, promoting the use of sintering mechanism resulting in a higher strength in the solid phase. The argument for using the consolidation kinetic was supported by special tests involving explosively loaded sand samples that were encapsulated within two assemblies approximating the thermal and pressure loading conditions of the two DOB cases [5,8]. The sand crushing and compacting have been confirmed in the corresponding conditions. The present model calculations are compared with CTH calculations employing the tabulated Sesame EOS model for Dry Sand [9] with the yield limit selected from the best fit of the ejecta shape [5] to the corresponding CTH calculations.

Thus, the present problem has been calculated with the present model using three yield limit descriptions for the condensed phase (low-Y; high-Y; and a variable Y managed by the sintering kinetic), and with the Sesame EOS model for Dry Sand. For further analysis, calculated target profiles are integrated into a single graph; for example, the 'Sintering' graph in figure 5 is composed from the target plate profiles taken from figure 4 at the time marks from table 1 and superimposed into a single picture. The results are summarized in figure 5 for the present model and in figure 6 for the Sesame

model. Figure 6, along with the Sesame EOS calculation, shows a summary of the experimental profiles and comparison of the variable-Y calculation (curve C) with the present experiment (curve E) at the last time mark of t = 540 μs.

An important characteristic for this problem, which is of major interest to experimentalists [3,4], is the vertical momentum transfer. The vertical displacement data taken from the present calculations are summarized in a single graph shown in figure 7. With possible experimental inaccuracies in mind shown by intervals in figure 7, it is seen that the best trend to the present experiment is observed for the calculation employing the sintering kinetic.

5. Discussion and conclusions

The shape of the sand ejecta can be well described by a variety of models. However, the mass and velocity distribution within the ejecta plays an important role in the deposition of momentum onto a target. Therefore, the internal mechanisms of the inter-phase exchange, which is generally believed to be relevant only for highly porous materials, are very important for the density distribution when ejecting soil even with conventional (moderate) porosity. The present calculations have demonstrated that taking the inter-phase exchange mechanisms into account might be important for evaluation of the momentum transfer. Evolution of strength of the porous material during its explosive consolidation and expansion was only superficially considered in the present publication. Further work on target effects, analysis of recovered samples and the effects of particle size and shape on the heat exchange and compaction kinetics is currently underway.

Summarising, the plate deformation and the vertical component of momentum deposited to the target plate in the present experiments are well described with the two-phase model. Managing the yield limit of the condensed phase of the sand through the sintering mechanism improves the description, but further study is necessary for evaluation of the material state and strength characteristics to be used in the analysis.

Acknowledgement

The authors are grateful to Mark Rausch, Jared Freundt, Steven Stojko, and Trevor Delaney, all of DSTO, for their assistance in conducting the experiments.

References

[1] Pickering E G, Chung Kim Yuen S and Nurick G N 2013 *Int. J. Impact Eng*. **58** 76
[2] Neubergera A, Peles S and Rittel D 2007 *Int. J. Impact Eng.* **34** 874
[3] Bergeron D M and Tremblay J E 2000 *Canadian Research to Characterise Mine Blast Output, 16th Int. MABS Symp.* (Oxford, UK)
[4] Taylor L C, Skaggs R R and Gault W 2005 *Fragblast* **9** 19
[5] Bergeron D, Walker R and Coffey C 1998 *Detonation of 100-Gram Anti-Personnel Mine Surrogate Charges In Sand - A Test Case For Computer Code Validation: Report DRES-668* (Ralston, Alberta, Canada: Defence Research Establishment Suffield)
[6] Resnyansky A D 2010 *J. Appl. Phys.* **108** 083534
[7] Resnyansky A D and Bourne N K 2004 *J. Appl. Phys.* **95** 1760
[8] Resnyansky A D 2012 *CTH Implementation of a Two-Phase Material Model With Strength: Application to Porous Materials: Report DSTO-TR-2728* (Edinburgh, Australia: Defence Science and Technology Organisation)
[9] Bell R L, Baer M R, Brannon R M, Crawford D A, Elrick M G, Hertel E S Jr., Schmitt R G, Silling S A and Taylor P A 2006 *CTH user's manual and input instructions version 7.1* (Albuquerque, NM: Sandia National Laboratories)
[10] http://www.sandia.gov/CTH/Release-leftnav-level1_js.html December 2, 2013
[11] Schwarz R B, Kasiraj P, Vreeland Jr T and Ahrens T J 1984 *Acta metall.* **32** 1243
[12] Simakov G V and Trunin R F 1990 *Izvestiya, Earth Physics* **26** 952